Reversion of epigenetically-mediated BIM silencing overcomes chemoresistance in Burkitt lymphoma

Jose A. Richter-Larrea[1], Eloy F. Robles[1], Vicente Fresquet[1], Elena Beltran[1], Antonio J. Rullan[1], M.ª José Calasanz[2], Carlos Panizo[3], Jose A. Richter[4], Xabier Agirre[1], Jesus M. Hernandez[5], Jose Roman-Gomez[6], Felipe Prosper[1,3], Jose A. Martinez-Climent[1]*

[1]Division of Oncology, Center for Applied Medical Research (CIMA), University of Navarra, Pamplona, Spain; [2]Department of Genetics, University of Navarra, Pamplona; [3]Hematology & Cell Therapy Programs, Clinica Universidad de Navarra, Pamplona; [4]Department of Nuclear Medicine, Clinica Universidad de Navarra, Pamplona; [5]Department of Hematology, Hospital Universitario and Center of Cancer Research, University of Salamanca-CSIC, Salamanca, Spain; and [6]Department of Hematology, Reina Sofia Hospital, Maimonides Institute for Biomedical Research, Cordoba, Spain

CORRESPONDING AUTHOR

*Jose A. Martinez-Climent, M.D., Ph.D., Division of Oncology, Center for Applied Medical Research (CIMA). University of Navarra. Avda Pio XII, 55. Pamplona 31008 (SPAIN). Tel: 34-948-194700-ext 1029; Fax: 34-948-194714; e-mail: jamcliment@unav.es

RUNNING TITLE: BIM-mediated chemoresistance in BL

MANUSCRIPT CONTENT: Word counts: text, 2.997; abstract, 200. Tables: 1; Figures: 5; References: 34. Supplementary information: Tables: 3; Figures: 4.

Presented in part as an oral communication at the 50th American Society of Hematology meeting (ASH), San Francisco, CA, USA, in December 2008; published in *Blood* (ASH Annual Meeting Abstracts), Nov 2008; 112: 607.

ABSTRACT

In Burkitt lymphoma/leukemia (BL), achievement of complete remission (CR) with first-line chemotherapy remains a challenging issue, as most patients who respond initially remain disease-free whereas those refractory have few options to be rescued with salvage therapies. The mechanisms underlying BL chemoresistance and how it can be circumvented are not completely known. Our previous integrative genomic analysis identified genetic and epigenetic inactivation of pro-apoptotic *BIM* gene in B-cell lymphomas. Here we show that *BIM* epigenetic silencing by concurrent promoter hypermethylation and deacetylation occurred frequently in primary BL samples and BL-derived cell lines. Remarkably, patients with hypermethylated *BIM* presented lower complete remission rate (24% *vs*. 79%;p=0.002) and shorter overall survival (p=0.007) than those with *BIM*-expressing lymphomas, indicating that *BIM* transcriptional repression may have mediated tumor chemoresistance. Accordingly, by combining *in vitro* and *in vivo* studies of human BL-xenografts grown in immunodeficient RAG2$^{-/-}$ IL2γc$^{-/-}$ mice and of mature B-cell lymphomas generated in Eμ-*MYC* and Eμ-*MYC*-*BIM*$^{+/-}$ transgenes, we demonstrate that chemoresistance is dictated by *BIM* gene dosage and that is reversible upon BIM reactivation by genetic manipulation or with histone-deacetylase inhibitors such as Vorinostat. We suggest that Vorinostat combined with high-dose chemotherapy may overcome chemoresistance, achieve durable remission and improve survival of patients with BL.

INTRODUCTION

Burkitt lymphoma/leukemia (BL) is a clinically aggressive B-cell malignancy accounting for between 85 and 90% of childhood and less than 5% of adult B-cell lymphomas in Europe and the United States. Three clinical variants are recognized by the WHO classification: sporadic, endemic or related to Epstein-Barr virus (EBV) infection, and human immunodeficiency virus (HIV)-associated.[1] Besides the typical cytologic and immunophenotypic findings, the characteristic hallmark of BL is the presence of chromosomal translocations deregulating *MYC* oncogene.[2] Clinically, the presence of older age, advanced tumor stage with bone marrow and leukemic disease, increased serum LDH and immunodeficiency have been correlated with poor outcome. However, there is not a clinical or biological marker able to predict responses to therapy.[3-6]

Current treatment for patients with BL includes multi-agent, dose-intensive chemotherapy regimens with central nervous system prophylaxis, which can achieve complete remission (CR) in around 90-95% of children and 60-70% of adults. The most critical issue in BL remains to achieve an initial CR, because those patients who respond to first-line chemotherapy have a high probability of remaining free of disease.[3,6,7] Conversely, patients who present primary chemoresistance or early relapse usually die early because of progressive disease or of therapeutic complications while attempting to achieve remission.[3,8] Salvage chemotherapy has been effective in up to one-third of children with refractory or relapsed BL, but no similar successful treatment has been reported for adults.[9]

Despite this clinical dilemma, the molecular basis of BL chemoresistance and, more importantly, how it can be circumvented, have not been elucidated.[10-13] We have previously reported that the gene encoding the pro-apoptotic BH3-only family member protein BIM is frequently inactivated by genetic and epigenetic abnormalities that vary substantially among the different B-cell lymphoma subgroups.[14] In some solid tumors and myeloid leukemias, BIM is commonly inactivated by post-transcriptional modifications that target it for degradation in the proteasome, leading to therapeutic resistance.[15-19] In addition, *BIM* is a suppressor of *MYC*-induced B-cell leukemias in mice.[20,21] However, whether *BIM* mediates chemotherapeutic resistance in mature B-cell lymphomas has not been addressed. In this report, we show that resistance to chemotherapy in patients with BL is dictated by the epigenetic silencing of *BIM*, and that this resistance can be reversed by reactivating BIM expression with histone deacetylase inhibitors (HDACis) such as the suberoylanilide hydroxiamic acid (SAHA, Vorinostat). Consequently, the combination of Vorinostat and high-dose chemotherapy may be of clinical benefit in patients with BL to prevent refractory disease.

MATERIALS AND METHODS

Burkitt lymphoma/leukemia primary biopsies and cell lines

Thirty-nine lymph node biopsies (n=12) or bone marrow aspirates (n=27) from HIV-negative Spanish patients diagnosed of Burkitt lymphoma/leukemia according to the World Health Organization (WHO) criteria and obtained before initiation of therapy were included in the study. Cases with atypical BL or with Burkitt-like lymphoma were excluded (Supplementary-Table 1). All evaluated lymphomas presented chromosomal translocations involving *MYC* gene: t(8;14)(q24;q32) (n=30), t(2;8)(p11;q24) (n=2) and t(8;22)(q24;q11) (n=3), detected by standard cytogenetics and/or fluorescence in situ hybridization (FISH). The four cases without evidence for *MYC* rearrangement presented karyotypes without mitosis and no material was available for FISH studies; however, a cytological, histological and immunophenotypic pattern characteristic of typical BL was observed in all of them. All patients received similar standard dose-intense chemotherapy including cyclophosphamide, anthracyclines, etoposide, vincristine, dexamethasone/prednisone, methotrexate and cytarabine, without rituximab, plus intrathecal prophylaxis.[22] Clinical and follow-up data was available for 36 of the 39 BL patients. In addition, twenty cell lines derived from patients with BL were studied, including Seraphina, Namalwa, Jijoye, Daudi, Elijah, Nab2, Raji and EB1 (EBV+); KHM10B, Wien133, Balm9, DG75, Ramos, BL2, BL41, CA46, Blue1, P32 and Tanoue (EBV-); and BL5, a cell line derived from a patient with HIV-associated BL (Supplementary-Table 2). The study was approved by the University of Navarra Institutional Review Board, and the clinical investigation was conducted according to Declaration of Helsinki principles.

Drugs

Suberoylanilide hydroxamic acid (SAHA, Vorinostat) was kindly provided by Merck & Co. laboratories (Rahway, NJ, USA). In addition, 5-aza-2-deoxycitidine and etoposide (Sigma-Aldrich, Steinheim, Germany); doxorubicin and cytarabine (Pfizer Inc, New York, USA), vincristine (Stada, Bad Vilbel, Germany), methotrexate and dexamethasone (Merck), we used.

Quantitative real-time polymerase chain reaction (QRT-PCR) and Western blot analyses

Measurement of the expression of *BIM* (ABI-Hs.00197982), *BAK* (ABI-Hs.00832876) and *BAX* (ABI-Hs.00180269) genes was performed with QRT-PCR using the assay-on-demand gene expression products in the ABI PRISM 7500 device (Applied Biosystems, Weitersadt, Germany). Expression levels were normalized with *GAPDH* (ABI-Hs.99999905) as an endogenous control. Expression of BCL2 family member proteins was studied by Western blotting in BL cell lines and primary biopsies. The following antibodies were used: Noxa (Oncogene Research Products, Boston, MA, USA); BIM, BAD, BID, BAK, BAX, MCL1 and BCL2 (Stressgen, Victoria, Canada), and Bcl-XL (Abcam, Cambridge, UK). To evaluate equal protein transfer, detection of Actin protein (Oncogene Research Products) was performed. To confirm homozygous deletion of *BIM* gene locus in two of the BL cell lines (P32 and BL2), PCR on genomic DNA was performed according to reported methods.[14]

Methylation analysis of *BIM* promoter sequences

Detection of hypermethylation of human *BIM* gene promoter by standard methylation-specific PCR (MSP) analysis was performed as previously reported.[14] In addition, *BIM* methylation levels were measured using quantitative real-time methylation-specific PCR (QRT-MSP) in a rapid fluorescent thermal cycler with three-color fluorescence monitoring capability (LightCycler, Roche), using 1 μL of bisulfite-modified DNA in 10 μl reaction volume with 0.4 μM each primer, and 1 μL of 10x LightCycler FastStar DNA Master SYBR Green I (Roche Molecular Biochemicals), as previously reported.[23]. For sequencing analysis of methylated areas, *BIM* promoter was amplified by nested-PCR after bisulfite modification. Amplification products obtained in the second PCR reaction were subcloned into pCR 4-TOPO plasmid using the TOPO TA Cloning Kit for Sequencing (Invitrogen Life Technologies, Paisley, UK) and transformed into *Escherichia coli* according to the manufacturer's recommendations. Colonies with recombinant plasmids containing the described PCR products were screened by digestion with *EcoRI* (Amersham Biosciences, Buckinghamshire, UK). Candidate plasmid clones were sequenced in the ABI 3730 Genetic Analyzer sequencer (Applied Biosystems). To evaluate demethylation, BL cell lines grown at a density of $3x10^5$ cells/mL in 25 cm^2 flasks with 10 mL of culture medium were treated with 2 μM of the demethylating agent 5-aza-2-deoxycitidine or 2 μM of Vorinostat; after incubation of 96 hours, cells were harvested for MSP, QRT-PCR, and Western blot analyses.

Quantitative Chromatin immunoprecipitation (ChIP)

BL cells were treated with 2 μM of Vorinostat for 48 h and subjected to ChIP. Quantitative PCR (Q-PCR) analysis of the ChIP fractions (10 ng) from antibody-bound and input chromatin was performed to assess the acetylated Histone 3 (AcH3; Upstate

Biotechnologies, Lake Placid, NY, USA) modification in canonical CpG island sequences of the BIM promoter. SYBR Green detection was used in the LightCycler platform (Roche, Basel, Switzerland). The amplification of the ChIP fraction and of the input DNA were used as a target and reference sequences, respectively. They were amplified in the same run using BIM-ChipD (5´-AGACCTTCCCCAGACTTGCT-3´) and BIM-ChipR (5´-TCTTTGCCCAGGACAGACTT-3´) primers. The same program conditions that for QRT-MSP were applied to perform Q-PCR-Chip, and calculations were also performed automatically by the LightCycler software (see above). The level of AcH3 was determined relative to input chromatin of each sample.

MYC and _P53_ gene sequencing analysis

Direct sequencing of *MYC* gene at box I and of *P53* (exons 4 to 8) was performed in the ABI 3730 sequencer, using the following primers: for *MYC* box I, forward, 5'-ACCTCGACTACGACTCGGTG-3'; reverse, 5'-AGAAGCCGCTCCACATACAG-3'. For *P53*: forward 5'- CTGCCGTCTTCCAGTTGC-3'; reverse 5'-TAAGCAGCAGGAGAAAGCCC-3' for exons 4 and 5; forward 5'-CGACAGAGCGAGATTCCATC-3'; reverse 5'- TCCCAAAGCCAGAGAAAAGA-3' for exon 6; forward 5'-GGTTGGGAGTAGATGGAGCC-3'; reverse 5'-CAAATGCCCCAATTGCAG-3' for exons 7 and 8.

Ectopic transfection of _BIM_ by retroviral transduction

Full-length *BIM (BCL2L11*) cDNA was cloned into the p-MIRG vector upstream from the internal ribosomal entry site (IRES) of the murine stem-cell virus (MSCV)–IRES–enhanced green fluorescent protein (GFP). p-MIRG-BIM and p-MIRG (empty vector) were transfected into Propack-A.52 cells (CRL-12479 ATCC, Manassas, VA, USA)

using lipofectamine (Invitrogen). Then, retroviral supernatant was collected and filtered through 0.45 µm filter. Titer of the p-MIRG-BIM and p-MIRG vectors was determined by infecting 3T3 cells (DSMZ, Braunschweig, Germany) in the presence of 8 µg polybrene (Sigma-Aldrich). For transduction of the BL cells, a 24-well plate was coated with 2 µg/mL of retronectin (Takara, Shuzo, Otsu, Japan) at 4ºC, overnight. After removal of the retronectin solution, the plate was blocked for 30 min at room temperature with sterile PBS containing 2% BSA. To pre-load the retrovirus into the plate, blocking solution was removed and 500 µL of retroviral supernatant was added and incubated at room temperature for 1 h. After three additional pre-load steps, 1 $x10^5$ cells were added to each well in RPMI/10% FBS containing 4 µg/mL polybrene (Sigma-Aldrich) and plates were then incubated at 37ºC under 5% CO_2. GFP positive cells were finally isolated using a FACSAria cell sorter (Beckton Dickinson Biosciences, San Jose, California, USA). Measurement of *BIM* expression levels was performed using QRT-PCR and Western blot analyses. Finally, single-cell clones were isolated from the BIM-expressing cell pools, and two of them presenting moderate and high expression levels of BIM (Seraphina clones 1 and 2, respectively) were selected for this study.

siRNA knockdown of BIM gene

BIM silencing was performed in two cell lines expressing BIM (KHM10B and Ramos) by transfection of three siRNAs (s195011, s195012 and s19474) and the Silencer Negative Control-1 siRNA (Ambion, Austin, TX, USA) using the Cell Line Nucleofector Solution V in a nucleofector device (Amaxa GmbH, Köln, Germany). After siRNA transfection, BIM protein expression was evaluated by Western blotting at 48 hours.

Citotoxicity and apoptosis assays

BL cells grown at a cell density of $1.2x10^6$ cells/4 mL were treated with doxorubicin, vincristine, methotrexate, cytarabine, etoposide and dexamethasone at 1, 5, 10 and 50 ng/mL, alone or in combination with 2 μM of Vorinostat during 24 hours or with 2 μM of 5-Aza during 72 hours. Cell viability was assessed by trypan-blue dye exclusion. To determine apoptosis, caspase 3 and 9 activation (with antibodies from BD Pharmingen and Stressgen, Victoria, BC, Canada, respectively) and PARP protein expression (with antibodies from Promega Corporation, Madison, WI, USA) were determined using Western blot. In addition, apoptosis was assessed by PS externalization using Annexin V/FITC in the presence of propidium iodide, and cell fluorescence was detected on a FACSCalibur using CellQuest Pro software, as reported.[24]

Establishment of BL xenografts in immunodeficient mice and *in vivo* therapy

All mouse experiments were performed in the Animal Core Facilities of CIMA (University of Navarra) after approval by the local Animal Ethics Committee. To evaluate whether BL cells with different BIM expression levels presented variable chemotherapy resistance *in vivo*, $2,5x10^6$ Seraphina cells transfected with p-MIRG (empty vector) or with p-MIRG-*BIM* clones 1 and 2, and wild-type cells were intravenously (i.v.) injected into immunodeficient $RAG2^{-/-}IL2\gamma c^{-/-}$ mice, which lack B, T, and NK cells.[25] Doxorubicin treatment was administered intraperitoneally (i.p.) on day 14 (10 mg/Kg body weight) and day 21 (5 mg/Kg body weight) after inoculation, whereas control mice received the corresponding vehicle (PBS). To test whether re-expression of BIM with Vorinostat therapy in BL cells was associated with modification of sensitivity to chemotherapy *in vivo*, $2,5\times10^6$ cells from wild-type Seraphina were i.v.

inoculated into RAG2$^{-/-}$IL2γc$^{-/-}$ recipients. Vorinostat treatment commencing 14 days after BL-cell inoculation was administered i.p. for 14 days (75 mg/Kg body weight), with or without doxorubicin (administered i.p. on days 14 and 21 after inoculation, 10 and 5 mg/Kg body weight, respectively). Control mice received the corresponding vehicle (DMSO). Mouse cohorts consisted of 5 to 8 mice each, and were clinically monitored and sacrificed when signs of tumor development were observed. To evaluate therapeutic efficacy at certain time points, mice were killed and enlarged lymph nodes and/or spleens were dissected, and apoptosis was evaluated as described above.

Positron Emission Tomography (PET) imaging of tumors in mice

To monitor tumor responses to chemotherapy *in vivo*, PET imaging was performed at certain time points in a dedicated small animal Philips Mosaic tomograph (Cleveland, Ohio, USA), with 2 mm resolution, 11.9 cm axial field of view (FOV) and 12.8 cm transaxial FOV. Mice were anesthetized with 2% isoflurane in 100% O_2 gas for ^{18}F-FDG injection (10 MBq ± 2.38 in 80-100 µL) in a tail vein, and were immediately awakened afterwards and placed back in the cage. Fifty minutes after radiotracer administration, animals were placed prone on the PET scanner bed to perform a static acquisition (sinogram) of 15 minutes under continuous anesthesia. Images were reconstructed using the 3D Ramla algorithm (a true 3D reconstruction) with 2 iterations and a relaxation parameter of 0.024 into a 128×128 matrix with a 1 mm voxel size applying dead time, decay, random and scattering corrections. For quantitative analysis of tumor 18 F-FDG uptake, regions of interest (ROIs) were drawn on coronal 1-mm-thick small-animal PET images. ROIs were drawn on several slices and finally, maximum standardized uptake value (SUVmax) was calculated for each

tumor using the formula SUV = tissue activity concentration/injected dose x body weight. SUVmax uptake expresses the glycolitic metabolism of tumor cells.

Lymphoma characterization, B-cell isolation and therapy of Eμ-*Myc* and *BIM*-deficient transgenes

Eμ-*Myc* transgenic mice (C57BL/6J-Tg-IghMyc-22Bri/J) and *BIM*$^{-/-}$ knock-out mice (C57BL/6J-Bcl2l11$^{tm1.1Ast}$/Bcl2l11$^{tm1.1Ast}$) were purchased from The Jackson laboratory (Bar Harbor, Maine, USA). Eμ-*Myc* mice were intercrossed with *BIM*$^{-/-}$ mice, and genotyping was performed to identify Eμ-*Myc*- *BIM*$^{+/-}$ and Eμ-*Myc*-*BIM*$^{-/-}$ mouse lines, as reported.[20] Transgenic mice were clinically monitored and killed upon overt signs of disease were observed. Lymphoma cells were harvested and cell suspensions were analyzed by flow cytometry using B220 and IgM antibodies (both from Becton Dickinson) to distinguish mature B-cell lymphomas (B220+IgM+) from pre-B-cell lymphomas (B220+IgM-). To test response to chemotherapy *in vitro*, primary B220+IgM+ tumor lymphocytes were incubated in IMDM with 20% inactivated FBS, 55μM of β-mercaptoethanol and 10μg/mL of anti-IgM for BCR-activation. After 12 hours, cells at a concentration of 2×10^6 cells/mL were treated for additional 12 hours with doxorubicin at a final concentration of 0.1μg/mL. Cell viability and apoptosis were evaluated as described above. To determine sensitivity of transgenic lymphomas to doxorubicin, 2.5x10^6 B220+IgM+ tumor lymphocytes obtained from *Eμ-Myc* or *Eμ-Myc-BIM*$^{+/-}$ mice were intravenously injected into RAG2$^{-/-}$IL2γc$^{-/-}$ mice. One week after inoculation, doxorubicin was administered i.p. (10 mg/Kg body weight), and tumor development was monitored and compared to control mice in the two transgenic subgroups.

Statistical analysis

To determine the statistical differences between cell viabilities, *p* values were calculated by using one-way ANOVA test followed by Levene test to assess the homogeneity of variances (HOV). The different post hoc multiple comparison tests used were: Tukey in the case of HOV or Tamhane in the absence of HOV (for comparisons with control group), and Dunnett (for multiple comparisons). Kaplan-Meier plots were depicted to evaluate overall survival (OS) of BL patients, xenografted mouse recipients and transgenic mice; 95% CI was computed using Kalbfleish-Prentice method. Associations between individual clinical and biological features and OS were determined using the log-rank (Mantle-Cox) test. The analyses were carried out using the SPSS 15.0 statistical software (SPSS Inc., Chicago, IL, USA) for Windows. For comparison between median values, Fischer exact test was used.

RESULTS

Epigenetic silencing of pro-apoptotic *BIM* correlates with chemoresistance in patients with Burkitt lymphoma/leukemia

Our previous integrative genomic and gene expression profiling study identified frequent homozygous deletion of *BIM* gene in mantle cell lymphoma. In addition, *BIM* promoter hypermethylation was detected in germinal center-derived B-cell lymphomas, including follicular lymphoma, diffuse large B-cell lymphoma and BL.[14] To expand this initial observation, we applied standard and quantitative methylation-specific PCR (MSP) and sequencing analyses of CpG islands of *BIM* gene promoter to BL samples, detecting *BIM* hypermethylation in 17 of 39 (46%) patient biopsies and in 15 of 18 (83%) cell lines (Figure 1A). Two additional BL cell lines, P32 and BL2, exhibited *BIM* gene inactivation by bi-allelic deletion (Figure 1B). Quantitative PCR analysis of chromatin immunoprecipitation (ChIP) fractions showed decrease of acetylated Histone 3 (AcH3) in canonical CpG island sequences of *BIM* promoter in hypermethylated cell lines but not in non-methylated tumors (Figure 1C). Concurrent *BIM* methylation and deacetylation were correlated with very low or absent RNA and protein expression levels (Figure 1D). Accordingly, treatment of methylated cells with the demethylating agent 5-Aza-2-deoxycitidine (5-Aza) or with the HDACi Vorinostat resulted in 1.5 to 4-fold BIM re-expression, while Vorinostat significantly increased AcH3 levels (Figures 1C and 1E). These data indicate that epigenetic silencing of *BIM* gene by both hypermethylation and deacetylation occurs frequently in BL and can be pharmacologically reversed. To investigate whether *BIM* hypermethylation was correlated with clinical features, we analyzed a series of 36 Spanish patients with BL who received similar intensive chemotherapeutic regimens plus central nervous

system prophylaxis.[22] Patient's clinical and laboratory data are shown in Table 1 and Supplementary-Table 1. All but four were adults and the median age was 39 years (range, 4-76). The majority (82%) presented extranodal involvement including bone marrow and leukemic disease (75%). Twenty-one of 36 patients (58%) achieved CR, resulting in a median OS of 15 months (95% confidence interval (CI): 0.4;29.5) (Figure 2A). *BIM* promoter hypermethylation was detected in 17 of 36 (47%) patient samples whereas 19 cases presented non-methylated *BIM* gene. At diagnosis, patients with methylated and unmethylated *BIM* were not distinguishable by the clinical and laboratory features typically associated with poor prognosis in BL (Table 1 and Supplementary-Figure 1A). However, patients with methylated *BIM* presented lower CR rate, as only 4 of 17 cases achieved CR *vs*. 15 of 19 patients in the unmethylated subgroup (24% *vs*. 79%; p=0.002). Accordingly, *BIM* hypermethylation was associated with shorter OS (median OS, 2 months *vs*. not reached; p=0.007) (Figure 2B and Supplementary-Figure 1B). Similar survival data were observed for patients under 50 years of age (Supplementary-Figure 1C). These data indicate that *BIM* transcriptional repression is correlated with chemotherapeutic resistance, leading to lower CR and shorter survival duration of patients with BL.

Biological features of BL cases with *BIM* hypermethylation

We explored whether *BIM* transcriptional silencing was correlated with EBV-infection status in BL cells. By quantitative MSP, higher hypermethylation levels of *BIM* gene were detected in EBV+ lymphomas compared to EBV- tumors (mean value, 91±13 *vs*. 35±22; p<0.01) (Figure 2C. In previous reports, box I *MYC* mutations targeting Pro-57 and Thr-58 enhanced MYC transformation and promoted B-cell lymphoma

development in mice by evading apoptosis as a result of a failure to induce BIM.[21,26] Direct sequencing revealed that box I MYC mutations spanning aminoacid positions 57 to 60 were more frequent in BL cells *BIM* hypermethylation than in non-methylated tumors (p=0.19) (Figure 2D and Supplementary-Figure 2A). Although statistical significance was not reached, these data suggest that *MYC* mutations may have played a role in the epigenetic silencing of *BIM*. Next, the expression of the BCL2-family member proteins, which are critical regulators of apoptosis in B-cell malignancies, was measured by Western blotting in BL samples. Tumors with unmethylated *BIM* presented a higher number of alterations in the BCL2-family proteins in comparison with the hypermethylated cell lines (Figure 2E). BAK and BAX proteins, two final effectors of the apoptotic cascades, presented null or very low expression in the unmethylated cell lines while showing normal expression at the RNA level, pointing out to a post-transcriptional mechanism as the putative cause of BAK/BAX down-regulation (Supplementary-Figure 2B). Additional studies revealed that only 2 of 9 primary hypermethylated BL biopsies showed *P53* mutations whereas these were detected in 6 of 15 non-methylated BL samples (22% *vs*. 40%; p=0.24) (Figure 2F). Together, these results indicate that transcriptional repression of *BIM* in BL cells may be sufficient to evade apoptosis, requiring a reduced number of lesions in other apoptotic regulatory proteins or in P53.[20,21] Therefore, BIM seems to function as a critical regulator of apoptosis in BL cells.

BL resistance to doxorubicin correlates with *BIM* expression levels

Patients with BL are currently treated with dose-intensive chemotherapy regimens including cyclophosphamide, doxorubicin, vincristine, methotrexate, etoposide,

dexamethasone and cytarabine.[3,4] To test whether BIM expression was correlated with differences in cytotoxicity profiles, Seraphina cell line, which exhibits complete *BIM* epigenetic silencing, was retrovirally transfected with a p-MIRG-*BIM* expressing vector (Figure 3A). Two Seraphina single-cell clones with elevated BIM expression (clone 1 with a 2-fold increase, and clone 2 with a 2.5-fold increase with respect to parental cells) were incubated with the chemotherapeutic agents. A statistically significant decrease in cell viability was observed with doxorubicin (which increased cytotoxicity rates 20-30% in comparison to control cells). However, these differences were not displayed with etoposide, methotrexate, cytarabine, dexamethasone and vincristine treatment (Figure 3A and Supplementary Figure 3). We could not test cyclophosphamide, as this drug is inactive until undergoes hepatic metabolism.[27] Treatment with doxorubicin induced cell death through the mitochondrial apoptotic pathway, as shown by activation of caspase 9 and increase of PARP (Figure 3B). Next, BIM was silenced using siRNA in BIM-expressing BL cell lines Ramos and KHM10B, which were incubated with the chemotherapeutic drugs. After doxorubicin treatment, cell viability was increased along with a decrease in apoptotic rates (roughly, 30-40%) in BIM-silenced cells in comparison to control cells (Figure 3C). These data indicate that selective resistance of BL cells to doxorubicin is partially conditioned by BIM expression levels. To test whether similar results could be observed *in vivo*, Seraphina clones 1 and 2 were i.v. inoculated into RAG2$^{-/-}$IL2γc$^{-/-}$ mice, which received doxorubicin or vehicle treatments. Mice carrying wild-type cells or cells transfected with the empty vector did not show differences in OS between treated and vehicle-treated subgroups. Conversely, mice injected with clones 1 and 2 receiving doxorubicin presented longer OS in comparison to vehicle-treated recipients, being these differences were more pronounced for mice carrying clone 2-derived

lymphomas (median OS, 32 *vs*. 22 days; p<0.001) than for those with clone 1 (29 *vs*. 25 days, p=0.01) (Figure 3D). Accordingly, reduction of lymphoma volumes and decreased glycolitic tumor activities were observed in recipients transplanted with clones 1 and 2 cells in comparison to control mice, as determined by PET imaging studies (Figure 3E). These data indicate that sensitivity to doxorubicin is correlated with BIM expression in BL xenografts *in vivo*, therefore expanding our previous observations *in vitro*.

BIM regulates chemoresistance in lymphomas developed in Eμ-*MYC* and *BIM*-deficient mice

A previous study demonstrated that *BIM*-mutant *Eμ-MYC* transgenic mice developed B-cell leukemias and lymphomas more efficiently than *Eμ-MYC* transgenes (Figure 4A and Supplementary-Figure 4).[20] We used this validated model to test whether BIM could condition sensitivity to chemotherapy in mouse B-cell lymphomas. First, mature B220+IgM+ tumor lymphocytes were isolated from *Eμ-MYC* or in *Eμ-MYC-BIM*$^{+/-}$ transgenes and treated with doxorubicin *ex vivo*. *Eμ-MYC* lymphoma cells showed decreased survival and higher apoptotic levels than *Eμ-MYC-BIM*$^{+/-}$ lymphoma cells after doxorubicin treatment (Figure 4B). To test this observation *in vivo*, 2.5x10^6 mature B220+IgM+ tumor lymphocytes isolated from six different lymphomas developed in *Eμ-MYC* or in *Eμ-MYC-BIM*$^{+/-}$ transgenes were injected i.v. into RAG2$^{-/-}$ IL2γc$^{-/-}$ recipients (Supplementary-Table 3). One week after inoculation, doxorubicin *vs*. vehicle-DMSO was administered (Figure 4C). After treatment and in comparison to DMSO-treated mice, mice carrying *Eμ-MYC* lymphomas presented an extended survival time of 30 days (median OS, 20 *vs*. 50 days; p=0.001) whereas those with *Eμ-MYC-BIM*$^{+/-}$ lymphomas only extended survival in 8 days (median OS, 40 *vs*. 48

days; p=0.03) (Figure 4D). Thus, mice *Eμ-MYC-BIM*$^{+/-}$ lymphomas were more resistant to chemotherapy than the *Eμ-MYC* subgroup *in vivo*. Moreover, at day 100 post-injection, four *Eμ-MYC* mouse recipients remain disease-free *vs*. only two in the *Eμ-MYC-BIM*$^{+/-}$ subgroup. Accordingly, PET studies showed a marked reduction in the glycolitic tumor activity in *Eμ-MYC* lymphoma-recipients in comparison to mice with *Eμ-MYC-BIM*$^{+/-}$ lymphomas after doxorubicin treatment (Figure 4E). These data confirm our previous results in a different mouse model, reinforcing the concept that *BIM* expression levels modulate chemosensitivity in *MYC*-driven lymphomas.

BL chemoresistance can be overcome by pharmacological re-expression of BIM

Last, to begin to translate these findings to the clinic, we tested whether resistance to chemotherapy was reversible upon pharmacological induction of BIM expression in BL-resistant lymphomas. Treatment of *BIM* epigenetically-silenced cell lines with 5-Aza induced a 1.5 to 2.5-fold up-regulation of *BIM* expression, while treatment with Vorinostat resulted in a 3.5 to 4-fold *BIM* re-expression (Figure 1E). Induction of BIM in BL cells was associated with a partial reversion of the resistance to doxorubicin *in vitro* along with an increase in the apoptotic rates, which were more pronounced for Vorinostat than for 5-Aza (Figure 5A). We therefore selected Vorinostat to explore whether similar results could be observed *in vivo*. Thus, 2.5×10^6 cells from wild-type Seraphina cell line (with complete *BIM* hypermethylation) were i.v. inoculated into four RAG2$^{-/-}$IL2γc$^{-/-}$ mouse cohorts that received Vorinostat, doxorubicin, Vorinostat plus doxorubicin, or vehicle (DMSO). Vorinostat was administered at low doses, enough to induce BIM expression without killing the lymphoma cells *in vitro* (data not shown). Accordingly, mice treated with DMSO presented similar survival duration than the Vorinostat-treated subgroup (median OS, 27 days). In contrast, doxorubicin-treated

mice presented longer survival (median OS, 33 *vs*. 27 days, $p<0.01$), but the Vorinostat and doxorubicin group had the longest OS (median OS, 37 *vs*. 27 days; $p<0.001$) (Figure 5B). Treatment of tumors with Vorinostat plus doxorubicin was associated with activation of the intrinsic apoptotic pathway (Figures 5C and 5D). Additionally, monitorization of tumor responses using PET imaging showed a marked reduction in tumor volume and glycolitic activity in mice treated with Vorinostat and doxorubicin in comparison to the other mouse cohorts (Figure 5E). These data indicate that the combination of Vorinostat at low doses (which allows re-expression of BIM thus sensitizing cells to chemotherapy) followed by doxorubicin was the optimal therapeutic in the xenograft model.

DISCUSSION

Our study demonstrates the power of coupling clinical investigation with experimental research to deal with a medical problem. We have used different *in vitro* assays and studies in human BL xenografts and transgenic mice to show that the epigenetic silencing of *BIM* is a critical mechanism of chemotherapy resistance in *MYC*-driven lymphomas. Accordingly, therapies that reactivate BIM function such as Vorinostat can reverse chemoresistance and enhance the efficacy of doxorubicin therapy in BL. Other studies aiming to evaluate the apoptosis and therapeutic activities of HDACis have been conducted in similar mouse models of lymphoma.[28,29] These and our report underline the importance of using appropriate experimental animal models for the pre-clinical evaluation of novel therapeutic agents, aiming to select optimal drug combinations to treat human disease.

This report includes a series of patients with aggressive Burkitt lymphoma/leukemia, as most of them were adults showing an extramedullary disease, mainly bone marrow involvement and leukemic dissemination.[3,4] Although our series may include more aggressive cases than other reported series of BL, the fact that almost half of our patients were refractory to initial chemotherapy allowed us to observe the correlation between the failure to achieve CR and the presence of *BIM* hypermethylation. We however believe that the percentage of such resistant cases with epigenetic silencing of *BIM* may be lower in other series of pediatric and adult BL patients.

BIM plays a central role in the therapeutic resistance of some solid tumors and myeloid leukemias, whereby BIM inactivation is caused by selective phosphorilation that targets it for degradation in the proteasome. This post-transcriptional BIM

inactivation mediated therapeutic resistance to tyrosine-kinase inhibitors in lung cancer,[30] MEK inhibitors in melanomas,[31] paclitaxel in epithelial tumors,[15] imatimib in chronic myeloid leukemia,[16] and sorafenib (a *RAF* kinase inhibitor) in acute myeloid leukemia.[32] Restoration of BIM expression with the proteasome inhibitor bortezomib or by mimicking its function with the BH3-mimetic ABT-737 reversed tumor chemoresistance.[15,16,30-32] Herein, we confirm the critical role of BIM in regulating chemoresistance but, differently to these reports, BIM inactivation occurred at the transcriptional level and not post-transcriptionally. This conclusion is of clinical relevance, because the reactivation of BIM function aiming to by-pass chemoresistance in BL should be performed with therapies such as demethylating agents or HDACis that can reverse the epigenetic silencing of BIM, and not with bortezomib of ABT-737 that could be used to treat solid tumors with BIM inactivation.

The data presented has prompted us to try to test the combination of Vorinostat with dose-intensive chemotherapy in patients with BL. Consequently, a phase I/II clinical trial has been recently approved by the Spanish cooperative group PETHEMA, with the end-point of determining the maximum tolerated dose and the therapeutic efficacy of Vorinostat in combination with rituximab and HyperCVAD in adult patients with refractory or early relapsed BL. Vorinostat as a single agent has been approved by the FDA in October 2006 for the treatment of progressive, persistent or recurrent cutaneous T-cell lymphoma after two prior systemic therapies, achieving clinical effective responses with an acceptable safety profile.[33] However, there is not extensive experience with Vorinostat in combination with chemo-immunotherapy in patients with mature B-cell lymphomas.[34] The results of several ongoing clinical trials (such as the NCT00667615 and NCT00601718; www.clinicaltrials.gob) and our own

experience will provide valuable information about the clinical effectiveness and toxicity profile of this drug combination in the treatment of patients with BL.

ACKNOWLEDGMENTS

We thank Drs. Martin Dyer (University of Leicester, Leicester, UK), William Harrington (University of Miami, Miami, USA) and James Stone (University of Alberta, Edmonton, Canada) for providing cell lines, Drs. Maria Collantes and Iván Peñuelas (University of Navarra) for mouse imaging studies, Dr. Marta García-Granero (University of Navarra) for support with the statistical studies, and Izaskun Sesma for excellent technical work with mice. This work was supported by the Spanish Ministry of Science and Innovation (grants PI081878 and RTICC-RD06/0020-0088/0111/0066/0006), the Navarra Government (Education and Health Councils), the CITTIL Spanish-French EU Program, and the UTE-CIMA project. J.A.R.-L. and E.B. are supported by pre-doctoral fellowships from the Spanish Ministry of Science and Innovation.

DISCLOSURES

No relevant conflicts of interest to declare.

AUTHORSHIPS

Jose A. Richter-Larrea: designed the study, performed most of the research of the manuscript, analyzed and interpreted the data
Eloy F. Robles: performed research, analyzed and interpreted data
Vicente Fresquet: performed research, analyzed and interpreted data
Elena Beltran: performed research, analyzed and interpreted data
Antonio J. Rullan: performed research, analyzed and interpreted data
M.ª José Calasanz: contributed samples, performed research
Carlos Panizo: contributed samples, performed research
Jose A. Richter: performed research, analyzed and interpreted data

Xabier Agirre: performed research, analyzed and interpreted data

Jesus M. Hernandez: contributed samples, performed research

Jose Roman-Gomez: contributed samples, performed research, analyzed and interpreted data

Felipe Prosper: contributed samples, analyzed and interpreted data

Jose A. Martinez-Climent: design the study, analyzed and interpreted data, wrote the manuscript

REFERENCES

1. Jaffe ES, Harris NL, Stein H, Isaacson PG. Classification of lymphoid neoplasms: the microscope as a tool for disease discovery. Blood. 2008;112:4384-4399.
2. Gelmann EP, Psallidopoulos MC, Papas TS, Dalla-Favera R. Identification of reciprocal translocation sites within the c-myc oncogene and immunoglobulin mu locus in a Burkitt lymphoma. Nature. 1983;306:799-803.
3. Blum KA, Lozanski G, Byrd JC. Adult Burkitt leukemia and lymphoma. Blood. 2004;104:3009-3020.
4. Yustein JT, Dang CV. Biology and treatment of Burkitt's lymphoma. Curr Opin Hematol. 2007;14:375-381.
5. Garcia JL, Hernandez JM, Gutierrez NC, et al. Abnormalities on 1q and 7q are associated with poor outcome in sporadic Burkitt's lymphoma. A cytogenetic and comparative genomic hybridization study. Leukemia. 2003;17:2016-2024.
6. Murphy SB, Fairclough DL, Hutchison RE, Berard CW. Non-Hodgkin's lymphomas of childhood: an analysis of the histology, staging, and response to treatment of 338 cases at a single institution. J Clin Oncol. 1989;7:186-193.
7. Levine AM. Challenges in the management of Burkitt's lymphoma. Clin Lymphoma. 2002;3 Suppl 1:S19-25.
8. Bociek RG. Adult Burkitt's lymphoma. Clin Lymphoma. 2005;6:11-20.
9. Griffin TC, Weitzman S, Weinstein H, et al. A study of rituximab and ifosfamide, carboplatin, and etoposide chemotherapy in children with recurrent/refractory B-cell (CD20+) non-Hodgkin lymphoma and mature B-cell acute lymphoblastic leukemia: a report from the Children's Oncology Group. Pediatr Blood Cancer. 2009;52:177-181.
10. Gutierrez MI, Cherney B, Hussain A, et al. Bax is frequently compromised in Burkitt's lymphomas with irreversible resistance to Fas-induced apoptosis. Cancer Res. 1999;59:696-703.
11. Valnet-Rabier MB, Challier B, Thiebault S, et al. c-Flip protein expression in Burkitt's lymphomas is associated with a poor clinical outcome. Br J Haematol. 2005;128:767-773.
12. Tafuku S, Matsuda T, Kawakami H, Tomita M, Yagita H, Mori N. Potential mechanism of resistance to TRAIL-induced apoptosis in Burkitt's lymphoma. Eur J Haematol. 2006;76:64-74.
13. Nomura Y, Yoshida S, Karube K, et al. Estimation of the relationship between caspase-3 expression and clinical outcome of Burkitt's and Burkitt-like lymphoma. Cancer Sci. 2008;99:1564-1569.
14. Mestre-Escorihuela C, Rubio-Moscardo F, Richter JA, et al. Homozygous deletions localize novel tumor suppressor genes in B-cell lymphomas. Blood. 2007;109:271-280.
15. Tan TT, Degenhardt K, Nelson DA, et al. Key roles of BIM-driven apoptosis in epithelial tumors and rational chemotherapy. Cancer Cell. 2005;7:227-238.
16. Kuroda J, Puthalakath H, Cragg MS, et al. Bim and Bad mediate imatinib-induced killing of Bcr/Abl+ leukemic cells, and resistance due to their loss is overcome by a BH3 mimetic. Proc Natl Acad Sci U S A. 2006;103:14907-14912.
17. Bouillet P, Metcalf D, Huang DC, et al. Proapoptotic Bcl-2 relative Bim required for certain apoptotic responses, leukocyte homeostasis, and to preclude autoimmunity. Science. 1999;286:1735-1738.

18. Bouillet P, Purton JF, Godfrey DI, et al. BH3-only Bcl-2 family member Bim is required for apoptosis of autoreactive thymocytes. Nature. 2002;415:922-926.
19. Enders A, Bouillet P, Puthalakath H, Xu Y, Tarlinton DM, Strasser A. Loss of the pro-apoptotic BH3-only Bcl-2 family member Bim inhibits BCR stimulation-induced apoptosis and deletion of autoreactive B cells. J Exp Med. 2003;198:1119-1126.
20. Egle A, Harris AW, Bouillet P, Cory S. Bim is a suppressor of Myc-induced mouse B cell leukemia. Proc Natl Acad Sci U S A. 2004;101:6164-6169.
21. Hemann MT, Bric A, Teruya-Feldstein J, et al. Evasion of the p53 tumour surveillance network by tumour-derived MYC mutants. Nature. 2005;436:807-811.
22. Oriol A, Ribera JM, Bergua J, et al. High-dose chemotherapy and immunotherapy in adult Burkitt lymphoma: comparison of results in human immunodeficiency virus-infected and noninfected patients. Cancer. 2008;113:117-125.
23. Roman-Gomez J, Cordeu L, Agirre X, et al. Epigenetic regulation of Wnt-signaling pathway in acute lymphoblastic leukemia. Blood. 2007;109:3462-3469.
24. Rubio-Moscardo F, Blesa D, Mestre C, et al. Characterization of 8p21.3 chromosomal deletions in B-cell lymphoma: TRAIL-R1 and TRAIL-R2 as candidate dosage-dependent tumor suppressor genes. Blood. 2005;106:3214-3222.
25. Traggiai E, Chicha L, Mazzucchelli L, et al. Development of a human adaptive immune system in cord blood cell-transplanted mice. Science. 2004;304:104-107.
26. Bhatia K, Huppi K, Spangler G, Siwarski D, Iyer R, Magrath I. Point mutations in the c-Myc transactivation domain are common in Burkitt's lymphoma and mouse plasmacytomas. Nat Genet. 1993;5:56-61.
27. de Jonge ME, Huitema AD, Rodenhuis S, Beijnen JH. Clinical pharmacokinetics of cyclophosphamide. Clin Pharmacokinet. 2005;44:1135-1164.
28. Lindemann RK, Newbold A, Whitecross KF, et al. Analysis of the apoptotic and therapeutic activities of histone deacetylase inhibitors by using a mouse model of B cell lymphoma. Proc Natl Acad Sci U S A. 2007;104:8071-8076.
29. Frew AJ, Lindemann RK, Martin BP, et al. Combination therapy of established cancer using a histone deacetylase inhibitor and a TRAIL receptor agonist. Proc Natl Acad Sci U S A. 2008;105:11317-11322.
30. Cragg MS, Kuroda J, Puthalakath H, Huang DC, Strasser A. Gefitinib-induced killing of NSCLC cell lines expressing mutant EGFR requires BIM and can be enhanced by BH3 mimetics. PLoS Med. 2007;4:1681-1689; discussion 1690.
31. Cragg MS, Jansen ES, Cook M, Harris C, Strasser A, Scott CL. Treatment of B-RAF mutant human tumor cells with a MEK inhibitor requires Bim and is enhanced by a BH3 mimetic. J Clin Invest. 2008;118:3651-3659.
32. Zhang W, Konopleva M, Ruvolo VR, et al. Sorafenib induces apoptosis of AML cells via Bim-mediated activation of the intrinsic apoptotic pathway. Leukemia. 2008;22:808-818.
33. Olsen EA, Kim YH, Kuzel TM, et al. Phase IIb multicenter trial of vorinostat in patients with persistent, progressive, or treatment refractory cutaneous T-cell lymphoma. J Clin Oncol. 2007;25:3109-3115.
34. Crump M, Coiffier B, Jacobsen ED, et al. Phase II trial of oral vorinostat (suberoylanilide hydroxamic acid) in relapsed diffuse large-B-cell lymphoma. Ann Oncol. 2008;19:964-969.

TABLE 1

Table 1	Clinical and Laboratory Characteristics of 36 Patients with BL			
	Whole series	BIM methylated	BIM unmethylated	
Number of patients	36	17 (47%)	19 (53%)	p value
Age (Years)				
Median	39	43	36	
Range	(4-76)	(6-76)	(4-68)	
<14 years	4 (11%)	1 (6%)	3 (16%)	0.6
Sex				
Male	24 (67%)	12 (71%)	12 (63%)	
Female	12 (33%)	5 (29%)	7 (37%)	0.73
Diagnosis				
Burkitt lymphoma	9 (25%)	5 (29%)	4 (21%)	0.71
Burkitt lymphoma-leukemia	27 (75%)	13 (76%)	14 (74%)	
Stage III/IV	34 (94%)	17 (100%)	17 (89%)	0.48
Bulky disease [1]	11 (32%)	4 (27%)	7 (37%)	0.71
Extranodal involvement [1]	28 (82%)	12 (80%)	16 (84%)	1
LDH level > 1000 IU [2]	21 (66%)	9 (69%)	12 (63%)	1
Complete remission	19 (53%)	4 (24%)	15 (79%)	0.002

(1) Data available on 34 patients)
(2) Data available on 32 patients

FIGURE LEGENDS

Figure 1. Epigenetic silencing of pro-apoptotic *BIM* gene in Burkitt lymphoma. (A) Standard MSP analysis of the *BIM* gene in BL-derived cell lines and patient samples (P1 and P2, unmethylated *BIM*; P3 and P4, methylated *BIM*) (top left). Quantitative analysis of methylation using quantitative MSP (bottom left), including cell lines with complete methylation according to standard MSP analysis (light grey), cell lines with partial methylation (dark grey), and unmethylated tumors (DG75, Tanoue and BALM9). PB: peripheral blood. Right: Sequencing analysis of the *BIM* promoter region after bisulfite modification. Black boxes indicate methylated cytosines while white boxes correspond to unmethylated cytosines in CpG dinucleotides. PB cells and BALM9 cell line (unmethylated), and the Seraphina cell line and a BL lymph-node biopsy from patient P4 (methylated), are shown. (B) Homozygous deletion of *BIM* gene in the EBV- P32 and BL2 cell lines, as revealed by a-CGH and PCR on tumor genomic DNA, resulting in null expression of BIM as shown by quantitative RT-PCR and Western blot analyses. (C) Quantitative ChIP assay of AcH3 binding to canonical CpG island sequences of *BIM* promoter in Vorinostat-treated and untreated cells. An increase of AcH3 levels after treatment with Vorinostat was detected in the hypermethylated Jijoye and Seraphina cell lines, but not in the unmethylated BALM9 cell line. (D) *BIM* epigenetic silencing was correlated with absent or low expression at RNA levels measured by QRT-PCR (top) and protein levels as determined by Western blot analysis (bottom) in BL derived cell lines and patient samples (P1 and P2, unmethylated *BIM*; P3, P4 and P5, methylated *BIM*). (E) Treatment with 5-Aza and

with Vorinostat restored BIM expression in methylated tumors at the RNA and protein levels.

Figure 2. Correlation of *BIM* epigenetic silencing with clinical outcome and with biological features in Burkitt lymphoma/leukemia. Kaplan-Meier curves for overall survival (OS) for (A) thirty-six patients with BL included in the study, and (B) for BL patients with methylated and unmethylated *BIM*, where *BIM* promoter hypermethylation was correlated with inferior CR rate (p=0.002) and shorter survival duration (p=0.007). (C) By MSP analysis, *BIM* hypermethylation was observed in eight EBV+ BL cell lines and in six of nine (66%) EBV- BL cell lines. By quantitative MSP analysis, measurement of *BIM* promoter hypermethylation according to EBV infection revealed higher hypermethylation levels in EBV+ lymphomas compared to EBV- tumors (p<0.01). (D) Correlation of box I *MYC* mutations in BL primary samples and cell lines with and without hypermethylation of *BIM*: mutations at box I from aminoacid position 57 to 60 (including Pro-57 and Thr-58 sites) were more frequent in BL cell lines and primary samples with *BIM* hypermethylation than in non-methylated tumors (12 of 24 cases, 50% *vs*. 6 of 16 cases, 37.5%; p=0.19). (E) Western blot analysis of BCL2 family proteins in BL cell lines, classified in methylated and unmethylated *BIM* subgroups. β-actin served as loading control. (F) Sequencing of *P53* gene identified a lower number of mutations in patient samples with hypermethylated *BIM* with respect to unmethylated samples. Because almost all BL cell lines carried *P53* mutations, this analysis was restricted to primary tumors.

Figure 3. Correlation of BIM expression levels with chemotherapy-induced apoptosis. (A) Seraphina cells were retrovirally transfected with p-MIRG-BIM and p-MIRG (empty vector). Single-cell clones were isolated from the BIM-expressing cell

pools. Using QRT-PCR and Western blot analyses, clones 1 and 2 showed intermediate and high BIM expression, respectively, with respect to the parental cell line. Seraphina clones 1 and 2 were incubated with individual chemotherapeutic agents, showing increased sensitivity to doxorubicin with respect to control cells, but not to other compounds tested (Supplementary Figure 3). (B) Chemotherapy treatment of clones 1 and 2 cells activated the intrinsic apoptotic pathway, through cleavage of caspase 9 and expression of PARP proteins, as determined by Western blot analysis. (C) Silencing of BIM by RNA interference in Ramos and KHM10B cell lines was correlated with an increase in the resistance profile to doxorubicin with respect to parental cell line and control (cells transfected with a scramble vector). (D) Kaplan-Meier survival curves of $RAG2^{-/-}IL2\gamma c^{-/-}$ mice transplanted with wild-type and genetically manipulated Seraphina cells, which received chemotherapy or vehicle after tumor inoculation. Mice injected with Seraphina-transfected clones 1 and 2 cells but not Seraphina wild-type or cells transfected with the empty vector presented a statistically significant prolonged OS after treatment with doxorubicin in comparison to vehicle-treated recipients. (E) Follow-up studies of tumor metabolic activity by micro PET performed two weeks after initiation of therapy revealed a better response after treatment in Seraphina clone 1 recipients than in clone 2 transplanted mice, whereas no response was observed in control mice carrying BL cells transfected with empty p-MIRG or parental wild-type cells. SUVmax, maximum standardized uptake value.

Figure 4. Lymphoma characterization, B-cell isolation and therapy of double *Eμ-Myc* and *BIM*-deficient transgenic mice. (A) Kaplan-Meier survival curves for *Eμ-MYC* and *Eμ-Myc-BIM*$^{+/-}$ mice. (B) Mature B220+IgM+ tumor lymphocytes isolated from *Eμ-MYC* and *Eμ-Myc-BIM*$^{+/-}$ mice were BCR-activated with anti-IgM and treated with doxorubicin. *Eμ-Myc* B220+IgM+ lymphoma cells showed decreased survival and

higher apoptotic levels than *Eμ-Myc-BIM*$^{+/-}$ B220+IgM+ lymphoma cells, according to annexin V/FITC staining. (C) Representative diagram of the experimental therapeutic design to test whether *Eμ-MYC* lymphoma cells were more sensitive than *Eμ-MYC-BIM*$^{+/-}$ lymphoma cells to doxorubicin treatment *in vivo*. (D) Kaplan-Meier survival curves for mice transplanted with mature B-cell *Eμ-Myc* and *Eμ-Myc-BIM*$^{+/-}$ lymphoma cells treated with doxorubicin *vs*. vehicle. In comparison to DMSO-treated mouse recipients, mice carrying *Eμ-Myc* lymphomas presented longer survival after therapy than those with *Eμ-Myc-BIM*$^{+/-}$ lymphomas. E) Micro-PET studies showed a significant reduction in the glycolitic tumor activity in *Eμ-Myc* lymphoma-recipients in comparison to mice with *Eμ-Myc-BIM*$^{+/-}$ lymphomas. PET studies were performed at day 7 (just before initiation of therapy) and at day 14 (one week after therapy).

Figure 5. Resistance to doxorubicin is reversible upon treatment with HDACis in human BL-xenografted mice. (A) Treatment of BL cells with 5-Aza or Vorinostat resulted in BIM re-expression (Figure 1E). Subsequent incubation of these cells with doxorubicin led to a higher decrease in cell viability in Seraphina and Jijoye cells treated with Vorinostat *vs*. 5-Aza therapy. (B) Experimental design and Kaplan-Meier survival curves for four mouse cohorts transplanted with Seraphina cells with *BIM* hypermethylation and treated with vehicle (DMSO), low-dose Vorinostat, doxorubicin, and low-dose Vorinostat plus doxorubicin. Those receiving the combination of Vorinostat and doxorubicin presented longer OS with respect to the other subgroups. (C) An increase in the apoptotic rates was observed upon treatment with Vorinostat and doxorubicin in Seraphina and Jijoye cells in comparison to other *in vitro* treatments, as determined by annexin V/PI staining. (D) Representative study of the induction of apoptosis in Seraphina cells after treatment with Vorinostat plus

doxorubicin, as shown by caspase 3 and 9 activation and increased PARP expression. (E) Micro PET studies showed that mice treated with Vorinostat plus doxorubicin presented a significant decreased in tumor activity in comparison to mice treated with Vorinostat or doxorubicin, which was correlated with prolonged survival. Images were taken two weeks after treatment with the corresponding compound.

Figure 1

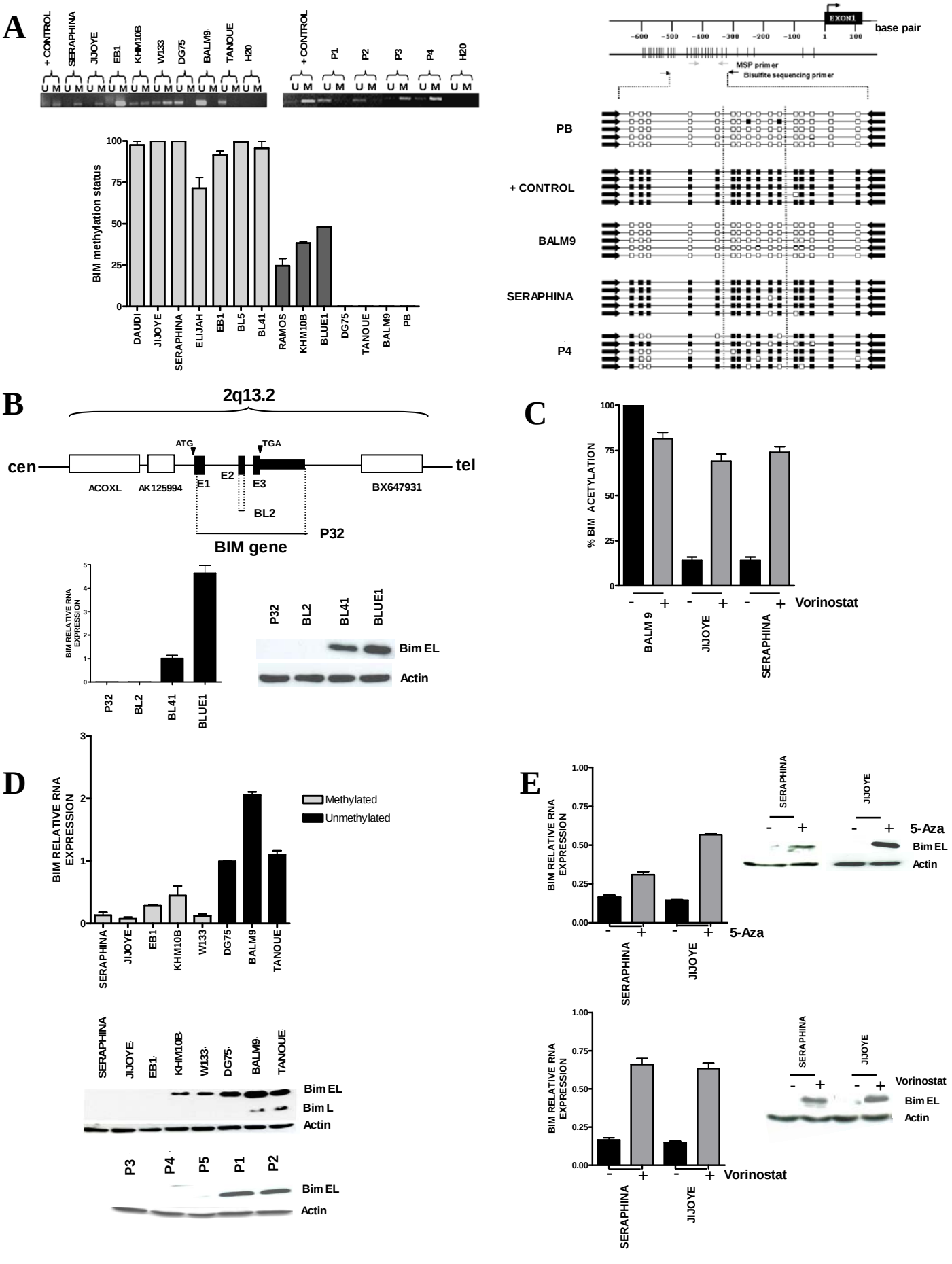
A
+ CONTROL
SERAPHINA
JIJOYE
EB1
KHM10B
W133
DG75
BALM9
TANOUE
H20
U M
+ CONTROL
P1
P2
P3
P4
H20
BIM methylation status
DAUDI
JIJOYE
SERAPHINA
ELIJAH
EB1
BL5
BL41
RAMOS
KHM10B
BLUE1
DG75
TANOUE
BALM9
PB
EXON1
base pair
MSP primer
Bisulfite sequencing primer
PB
+ CONTROL
BALM9
SERAPHINA
P4
B
2q13.2
cen
tel
ATG
TGA
ACOXL
AK125994
E1
E2
E3
BX647931
BL2
P32
BIM gene
BIM RELATIVE RNA EXPRESSION
P32
BL2
BL41
BLUE1
Bim EL
Actin
C
% BIM ACETYLATION
Vorinostat
BALM 9
JIJOYE
SERAPHINA
D
BIM RELATIVE RNA EXPRESSION
Methylated
Unmethylated
SERAPHINA
JIJOYE
EB1
KHM10B
W133
DG75
BALM9
TANOUE
Bim EL
Bim L
Actin
P3
P4
P5
P1
P2
Bim EL
Actin
E
BIM RELATIVE RNA EXPRESSION
5-Aza
SERAPHINA
JIJOYE
Bim EL
Actin
BIM RELATIVE RNA EXPRESSION
Vorinostat
SERAPHINA
JIJOYE
Bim EL
Actin

Figure 2

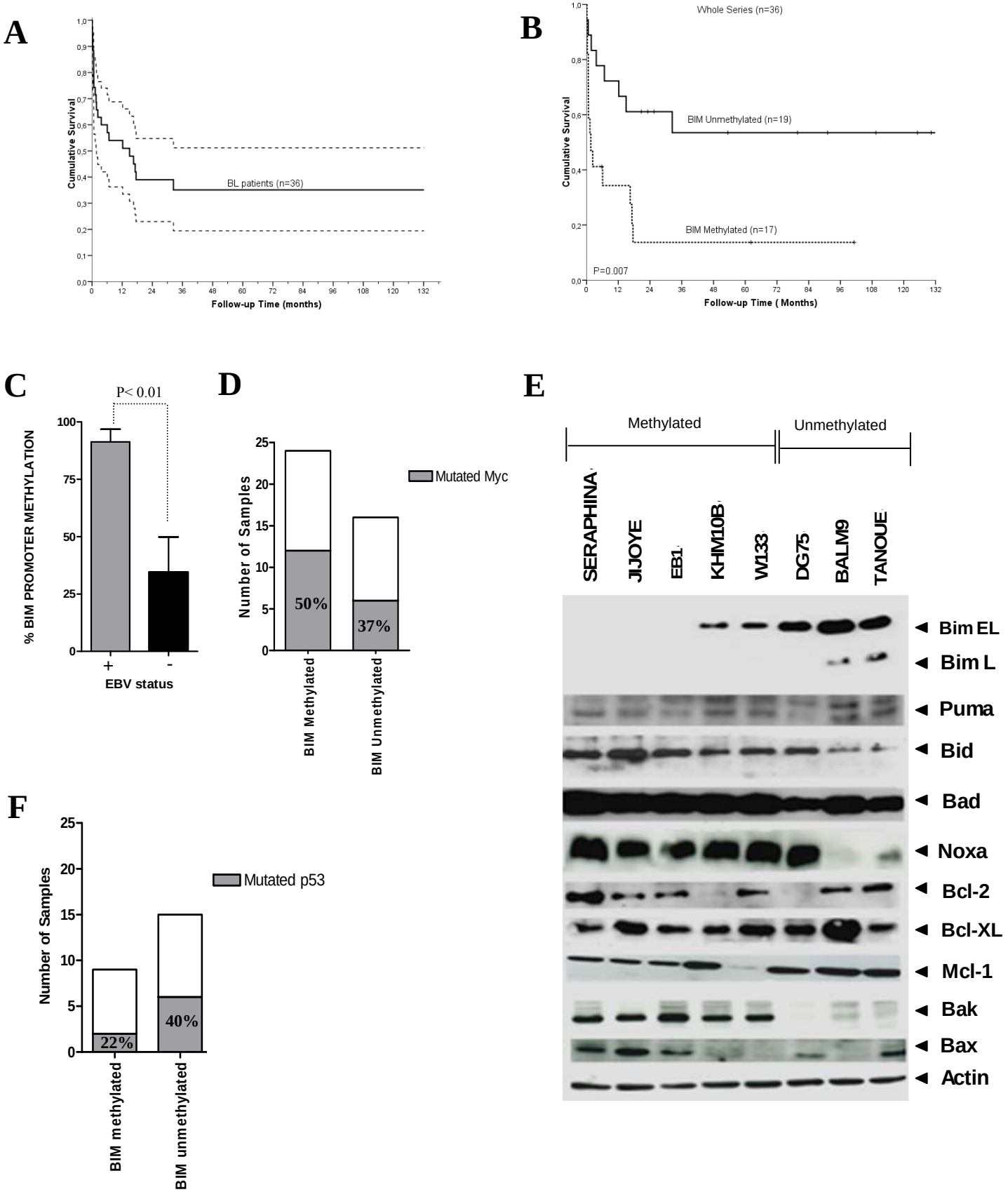
A
Cumulative Survival
BL patients (n=36)
Follow-up Time (months)
B
Whole Series (n=36)
BIM Unmethylated (n=19)
BIM Methylated (n=17)
P=0.007
Cumulative Survival
Follow-up Time (Months)
C
P< 0.01
% BIM PROMOTER METHYLATION
EBV status
D
Mutated Myc
Number of Samples
50%
37%
BIM Methylated
BIM Unmethylated
E
Methylated
Unmethylated
SERAPHINA
JIJOYE
EB1
KHM10B
W133
DG75
BALM9
TANOUE
Bim EL
Bim L
Puma
Bid
Bad
Noxa
Bcl-2
Bcl-XL
Mcl-1
Bak
Bax
Actin
F
Mutated p53
Number of Samples
22%
40%
BIM methylated
BIM unmethylated

Figure 3

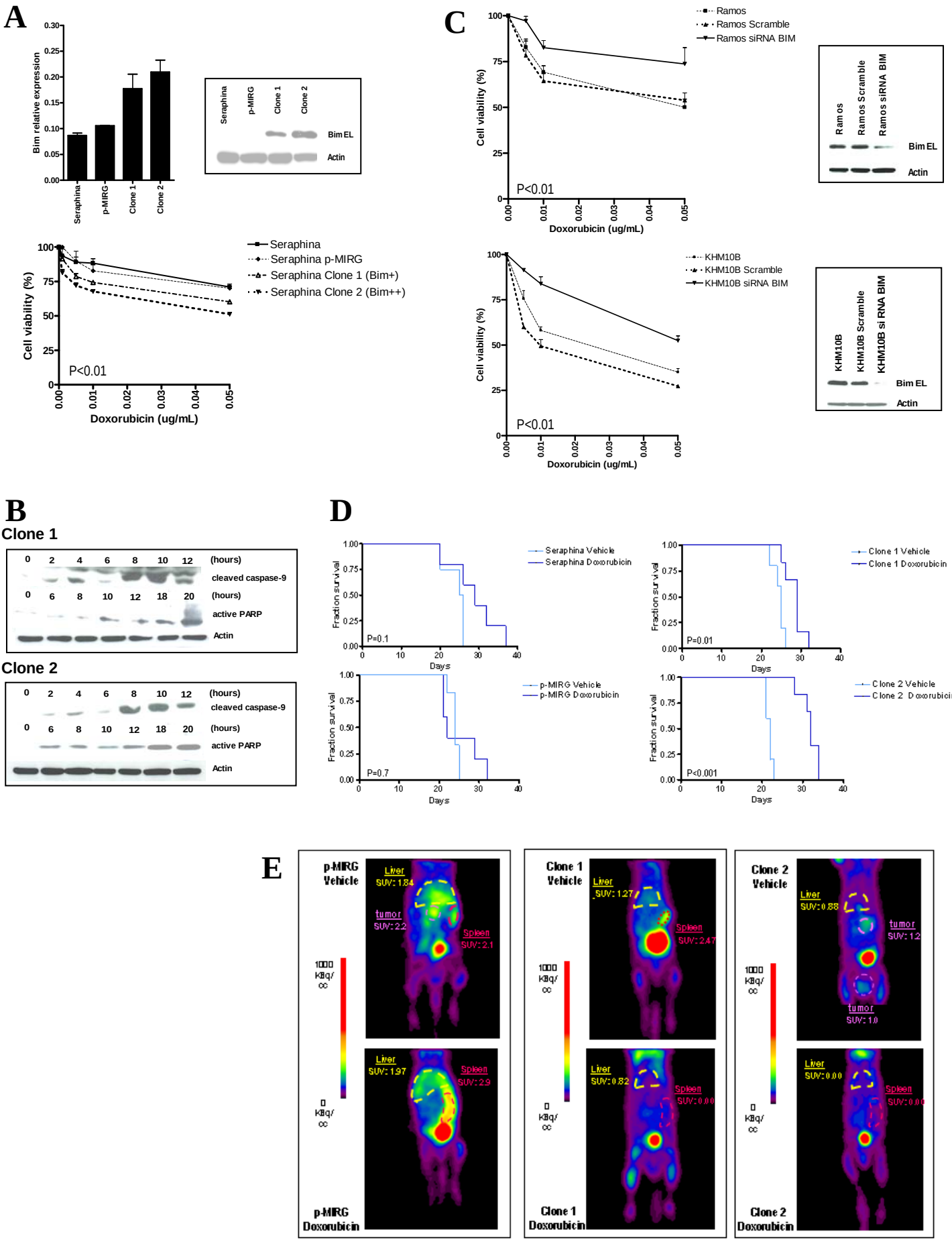
A
Bim relative expression
Seraphina
p-MIRG
Clone 1
Clone 2
Bim EL
Actin
Cell viability (%)
Seraphina
Seraphina p-MIRG
Seraphina Clone 1 (Bim+)
Seraphina Clone 2 (Bim++)
P<0.01
Doxorubicin (ug/mL)
C
Ramos
Ramos Scramble
Ramos siRNA BIM
KHM10B
KHM10B Scramble
KHM10B si RNA BIM
B
Clone 1
Clone 2
(hours)
cleaved caspase-9
active PARP
Actin
D
Seraphina Vehicle
Seraphina Doxorubicin
Clone 1 Vehicle
Clone 1 Doxorubicin
p-MIRG Vehicle
p-MIRG Doxorubicin
Clone 2 Vehicle
Clone 2 Doxorubicin
Fraction survival
Days
P=0.1
P=0.01
P=0.7
P<0.001
E
p-MIRG Vehicle
Clone 1 Vehicle
Clone 2 Vehicle
p-MIRG Doxorubicin
Clone 1 Doxorubicin
Clone 2 Doxorubicin
Liver
tumor
Spleen
SUV: 1.84
SUV: 2.2
SUV: 2.1
SUV: 1.97
SUV: 2.9
SUV: 1.27
SUV: 2.47
SUV: 0.82
SUV: 0.88
SUV: 1.2
SUV: 1.0
SUV: 0.00
1000 kBq/cc
0 kBq/cc

Figure 4

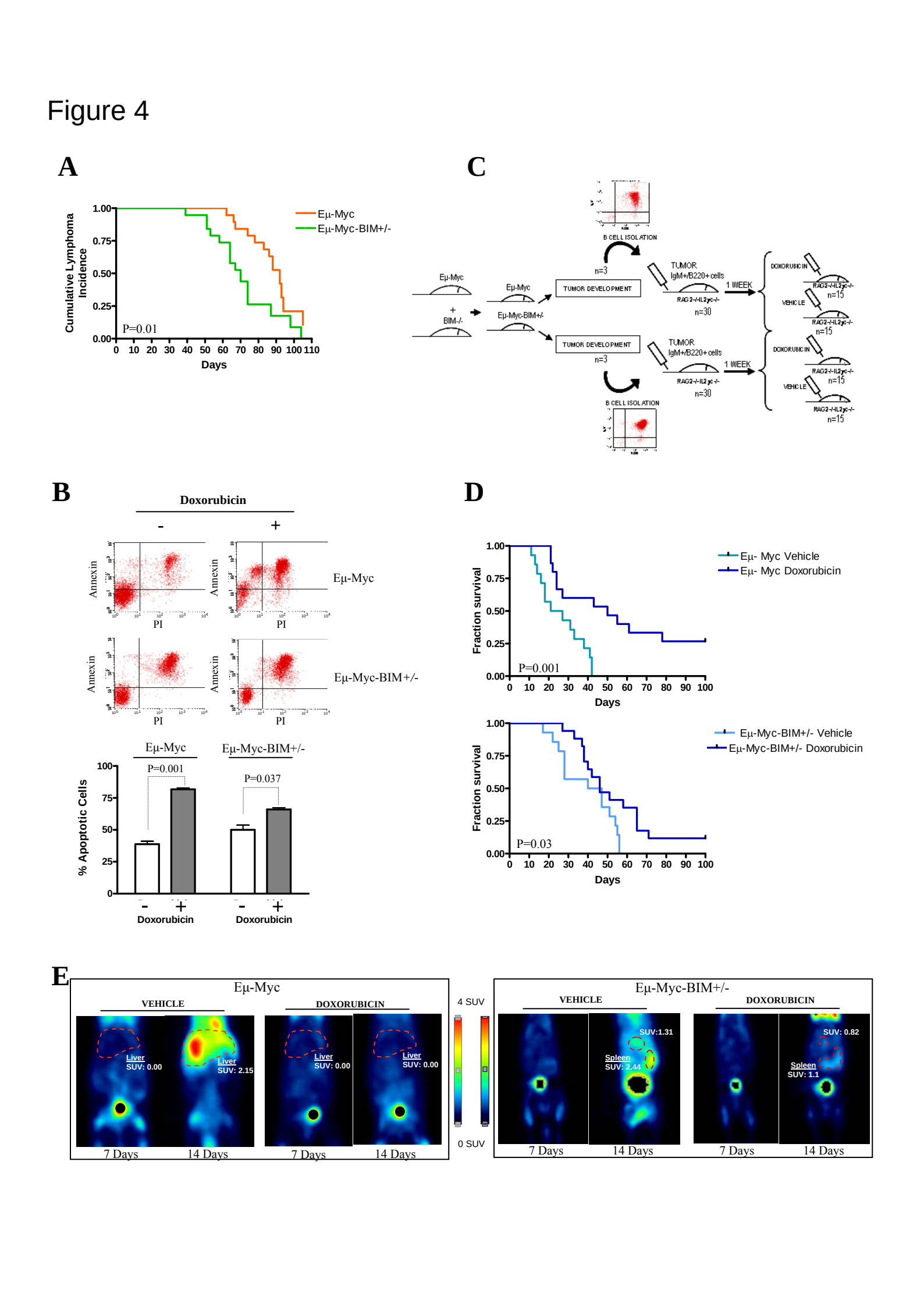
A
Cumulative Lymphoma Incidence
1.00
0.75
0.50
0.25
0.00
0 10 20 30 40 50 60 70 80 90 100 110
Days
P=0.01
Eμ-Myc
Eμ-Myc-BIM+/-
C
Eμ-Myc
+
BIM-/-
Eμ-Myc
Eμ-Myc-BIM+/-
TUMOR DEVELOPMENT
TUMOR DEVELOPMENT
n=3
n=3
B CELL ISOLATION
B CELL ISOLATION
TUMOR IgM+/B220+ cells
TUMOR IgM+/B220+ cells
RAG2-/-IL2rγc-/-
n=30
RAG2-/-IL2rγc-/-
n=30
1 WEEK
1 WEEK
DOXORUBICIN
VEHICLE
DOXORUBICIN
VEHICLE
RAG2-/-IL2rγc-/-
n=15
B
Doxorubicin
-
+
Annexin
PI
Eμ-Myc
Eμ-Myc-BIM+/-
% Apoptotic Cells
100
75
50
25
0
P=0.001
P=0.037
Eμ-Myc
Eμ-Myc-BIM+/-
- + - +
Doxorubicin
Doxorubicin
D
Fraction survival
1.00
0.75
0.50
0.25
0.00
0 10 20 30 40 50 60 70 80 90 100
Days
P=0.001
Eμ- Myc Vehicle
Eμ- Myc Doxorubicin
P=0.03
Eμ-Myc-BIM+/- Vehicle
Eμ-Myc-BIM+/- Doxorubicin
E
Eμ-Myc
VEHICLE
DOXORUBICIN
Liver
SUV: 0.00
Liver
SUV: 2.15
Liver
SUV: 0.00
Liver
SUV: 0.00
7 Days
14 Days
7 Days
14 Days
4 SUV
0 SUV
Eμ-Myc-BIM+/-
VEHICLE
DOXORUBICIN
SUV:1.31
Spleen
SUV: 2.44
SUV: 0.82
Spleen
SUV: 1.1
7 Days
14 Days
7 Days
14 Days

Figure 5

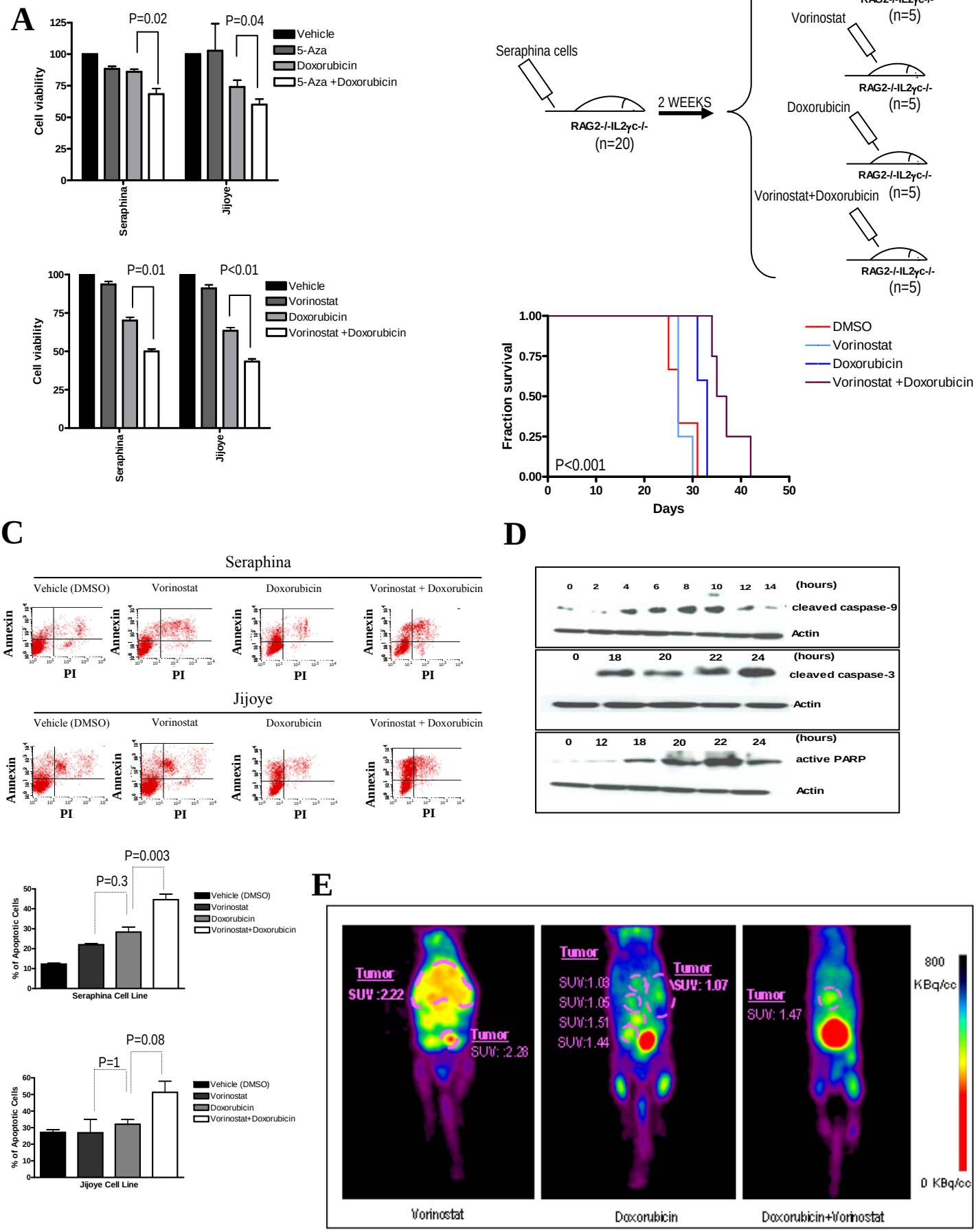
A
P=0.02
P=0.04
Vehicle
5-Aza
Doxorubicin
5-Aza +Doxorubicin
Cell viability
Seraphina
Jijoye
P=0.01
P<0.01
Vorinostat
Vorinostat +Doxorubicin
B
Seraphina cells
RAG2-/-IL2γc-/-
(n=20)
2 WEEKS
Vehicle
Vorinostat
Doxorubicin
Vorinostat+Doxorubicin
(n=5)
Fraction survival
P<0.001
Days
DMSO
C
Seraphina
Vehicle (DMSO)
Vorinostat
Doxorubicin
Vorinostat + Doxorubicin
Annexin
PI
Jijoye
P=0.003
P=0.3
% of Apoptotic Cells
Seraphina Cell Line
P=0.08
P=1
Jijoye Cell Line
D
(hours)
cleaved caspase-9
Actin
cleaved caspase-3
active PARP
E
Tumor
SUV :222
SUV: 2.28
SUV:1.08
SUV:1.05
SUV:1.51
SUV:1.44
SUV: 1.07
SUV: 1.47
800
KBq/cc
0 KBq/cc
Vorinostat
Doxorubicin
Doxorubicin+Vorinostat